Energies and Lifetimes of Magnons in Complex Ferromagnets: A First-Principle Study of Heusler Alloys

Paweł Buczek,[1,*] Arthur Ernst,[1] Patrick Bruno,[1,2] and Leonid M. Sandratskii[1]
[1]*Max-Planck-Institut für Mikrostrukturphysik, Weinberg 2, 06120 Halle, Germany*
[2]*European Synchrotron Radiation Facility – BP 220,38043 Grenoble Cedex, France*
(Received 26 March 2009; published 19 June 2009)

The energies and lifetimes of magnons in several Mn-based Heusler alloys are studied using linear response density functional theory. The number of the spin wave branches in Co_2MnSi corresponds to the number of its magnetic sublattices in contrast with the NiMnSb case in which the induced Ni sublattice cannot support optical magnons. The half-metallicity of these systems results in long-living acoustic spin waves. The example of non-half-metallic Cu_2MnAl shows that the hybridization with Stoner continuum leads not only to the damping of magnons but also to a renormalization of their energies.

DOI: 10.1103/PhysRevLett.102.247206 PACS numbers: 75.30.Ds, 75.40.Gb, 75.47.Np

Spintronics [1] is expected to deliver future generations of low-power computers. While its semiconductor sector struggles with the fabrication of materials ferromagnetic at room temperature, high-temperature metal-based spintronics is now well established, particularly in magnetic storage technologies taking advantage of giant magnetoresistance [2]. An important class of materials for spintronics applications is half-metals (HMs), especially Heusler phases [3,4]. In these complex systems one of the spin channels is semiconducting, while the other is metallic, which results in full polarization of carriers at the Fermi level and allows construction of efficient spin-valve devices. A substantial effort has been devoted to the study of spin-flip excitations in Heusler alloys, since the excitations determine the temperature dependence of magnetic properties and the Curie temperature. They can influence the operation of ever smaller and faster spintronic devices. In this Letter we consider spin-flip excitations of three Heusler alloys from the perspective of a first-principles theory. The materials are promising candidates for applications in spintronic devices.

In a ferromagnetic system there are two major mechanisms leading to a change of net magnetic moment. First is the single-electron spin-flip (Stoner) excitation, in which an electron is promoted from an occupied state with a given spin projection to an empty state with an opposite spin projection. The second type are so-called spin waves (SW), which are collective excitations of the electron system often visualized as a coherent precession of atomic moments.

On the theoretical side most of the parameter-free studies of the SW excitations are based on the mapping of itinerant electron systems on an effective Heisenberg spin-Hamiltonian [5]. This so-called adiabatic approach is very efficient and in many cases provides a good description of the available experimental data. Unfortunately, it neglects completely the influence of the Stoner excitations on the characteristics of the SWs. Therefore the major attenuation mechanism of SW in metallic magnets, usually referred to as Landau damping, is not taken into account. A method allowing a parameter-free study of both the energies and lifetimes of the SW is based on the analysis of the transverse dynamic magnetic susceptibility within the linear response density functional theory (LRDFT) [6,7].

Despite the commonly accepted usefulness and importance of this approach, only very few LRDFT studies of the dynamic magnetic susceptibility exist. They deal only with elementary bulk systems, since the extension of such calculations to more complex systems is computationally demanding. In this Letter we report the first LRDFT study of the dynamic magnetic susceptibility of multisublattice systems. We consider Heusler alloys Cu_2MnAl, NiMnSb, and Co_2MnSi, which differ in the number of magnetic sublattices and therefore in the number of expected SW branches. Additionally two of the systems (NiMnSb and Co_2MnSi) are half-metallic and allow us to explore the relation between SW properties and half-metallicity.

We first outline the LRDFT scheme used. Two types of response functions are considered: the Kohn-Sham (KS) (unenhanced) susceptibility χ_{KS} and true (enhanced) susceptibility χ. χ_{KS} describes the non-self-consistent response of a KS system to the transverse time-dependent magnetic field. Since the induced magnetization leads to a change of the exchange-correlation potential experienced by the electrons, the problem must be solved self-consistently in order to obtain χ. The relation between χ and χ_{KS} is described by the so-called susceptibility Dyson equation. For a given frequency nonzero eigenvalues of the loss tensor, $-\frac{i}{2}(\chi - \chi^{\dagger})$, where χ is the retarded susceptibility, signify the presence of complex singularities of χ and thus excited magnetic states. The corresponding eigenvectors determine the shapes of the excitations.

We use a discrete translational invariance of the systems and define a spatiotemporal Fourier transformation $f(\mathbf{r}, \mathbf{q}, \omega) = \sum_{\mathbf{R}} \int_{-\infty}^{\infty} dt f(\mathbf{r} + \mathbf{R}, t) e^{i(\omega t - \mathbf{q}\cdot\mathbf{R})}$, where the summation proceeds over crystal lattice and $\mathbf{r}$ belongs to

the Wigner-Seitz cell Ω of the crystal. $\mathbf{q}$ is a vector in the first Brillouin zone (BZ) Ω_{BZ}. The retarded susceptibility $\chi^{ij}(\mathbf{r}, \mathbf{r}', \mathbf{q}, \omega)$ relates the components of the external magnetic field and the induced magnetization, $\Delta m^i(\mathbf{r}, \mathbf{q}, \omega) = \sum_j \int_\Omega d\mathbf{r}' \chi^{ij}(\mathbf{r}, \mathbf{r}', \mathbf{q}, \omega) B^j(\mathbf{r}', \mathbf{q}, \omega)$. In this Letter we consider magnets with a collinear ground state and assume that the ground state magnetization $\mathbf{m}(\mathbf{r})$ points everywhere along the z direction. Similarly, the ground state xc magnetic field has only a z component, $B_{\mathrm{xc}}(\mathbf{r})$. No *external static* magnetic field is considered along the z direction. The collinearity implies that the spectrum of the spin-flip processes is determined by $\chi^+ \equiv \chi^{xx} + i\chi^{xy}$ and the response to the transverse (i.e., in the xy plane) magnetic field is transverse. In this case the Dyson equation assumes the following form:

$$\chi^+(\mathbf{r}, \mathbf{r}', \mathbf{q}, \omega) = \chi^+_{\mathrm{KS}}(\mathbf{r}, \mathbf{r}', \mathbf{q}, \omega) + \int_\Omega d\mathbf{r}_1 \chi^+_{\mathrm{KS}}(\mathbf{r}, \mathbf{r}_1, \mathbf{q}, \omega) \times K_{\mathrm{xc}}(\mathbf{r}_1)\chi^+(\mathbf{r}_1, \mathbf{r}', \mathbf{q}, \omega). \quad (1)$$

We have adopted here the adiabatic local density approximation (ALDA) to the exchange-correlation (xc) kernel K_{xc} describing the change of xc potential due to the induced magnetization. In this approximation the kernel is frequency independent and in the equation for the transverse susceptibility reduces to $K_{\mathrm{xc}}(\mathbf{r}) = B_{\mathrm{xc}}(\mathbf{r})/m(\mathbf{r})$. To make the calculation numerically efficient we adopt Matsubara formalism [8] and calculate the susceptibility at the Matsubara frequencies $i\omega_n^b = i2\pi nT$ at the imaginary axis and then perform an analytical continuation to the real frequency axis. $\chi^+_{\mathrm{KS}}(\mathbf{r}, \mathbf{r}', \mathbf{q}, i\omega_n^b)$ is found as the autoconvolution of the Korringa-Kohn-Rostoker Green's function

$$\chi^+_{\mathrm{KS}}(\mathbf{r}, \mathbf{r}', \mathbf{q}, \omega) = T \sum_{m \in \mathbb{Z}} \int_{\mathrm{BZ}} \frac{d\mathbf{k}}{\Omega_{\mathrm{BZ}}} G_\uparrow(\mathbf{r}, \mathbf{r}', \mathbf{q} + \mathbf{k}, z_m) \times G_\downarrow(\mathbf{r}', \mathbf{r}, \mathbf{k}, z_{m-n}), \quad (2)$$

where $z_m = \epsilon_F + i(2m + 1)\pi T$, ϵ_F is Fermi energy and the Green's function is determined as the lattice Fourier transform of the resolvent of the self-consistent Kohn-Sham equation $(z - H^\sigma_{\mathrm{KS}}(\mathbf{x}))G_\sigma(\mathbf{x}, \mathbf{x}', z) = \delta(\mathbf{x} - \mathbf{x}')$, where H^σ_{KS} is the KS Hamiltonian evaluated on the self-consistent ground state. $\sigma = \uparrow, \downarrow$ denotes the spin up and spin down channels. A similar approach was applied in Ref. [8] to study paramagnetic susceptibility of elementary metals. To solve the Dyson equation we use a basis, in which the angular dependence of the susceptibility in a given atomic cell is expanded into spherical harmonics and the radial dependence into Chebyshev polynomials. Such a choice greatly improves numerical stability and efficiency, allowing to perform many operations analytically. Equation (1) can be simply solved by a matrix inversion. The use of the KKR Green's function, Matsubara formalism, and the analytic basis are particularly important for the efficient description of multisublattice materials. It also allows the study of systems with reduced translational symmetry, in particular, thin magnetic films [9]. The computer code can be effectively parallelized.

χ^+_{KS} describes spin-flip transitions between occupied and empty KS states which form the Stoner continuum. The loss tensor associated with χ^+ can develop a peak outside the continuum, providing that the matrix $1 - \chi^+_{\mathrm{KS}}K_{\mathrm{xc}}$ becomes singular for a certain frequency. This new type of the excitation of the system—spin wave—appears as a collective response of the electron system to the applied magnetic field. Since the Landau damping is the only broadening mechanism in the ALDA the SWs outside the Stoner continuum have well defined energy. They should be particularly easy to detect in half-metals, where Stoner states acquire a finite activation energy $\gamma_S = E_b - \epsilon_F$, E_b standing for the bottom energy of the valence band in the channel featuring the half-metallic gap. For magnons with energies below γ_S the Landau mechanism is inoperative. SWs appearing in the Stoner continuum acquire finite lifetime due to the hybridization with Stoner sates. The frequency dependence of the corresponding eigenvalues can be well described by a Lorentzian $\chi^+_\lambda(\mathbf{q}, \omega) \approx A_\lambda(\mathbf{q})/((\omega - \omega_{0\lambda}(\mathbf{q}))^2 + \beta_\lambda(\mathbf{q})^2)$. $\omega_{0\lambda}$ is the SW energy, while β_λ can be interpreted as the inverse lifetime of the state.

Full Heusler compound Co_2MnSi [10] features a large 0.419 eV half-metallic gap in spin minority channel and $\gamma_S = 55$ meV. An example of the calculated loss tensor spectrum is presented in Fig. 1: three clear SW peaks can be discerned. The energies and inverse lifetimes of the SWs along main directions in BZ are presented in Fig. 2(a) and 2(b). The lowest mode ("acoustic" or EV 1) has vanishing energy for $\mathbf{q} = \mathbf{0}$. This is a manifestation of the spin rotational invariance preserved rigorously in the scheme. (This so-called Goldstone mode appears due to the absence of magnetic anisotropy.) As expected, the width of EV 1 is zero within the numerical noise for $\omega_{01}(\mathbf{q}) < \gamma_S$. Somewhat surprisingly, $\beta_1(\mathbf{q})$ does not ex-

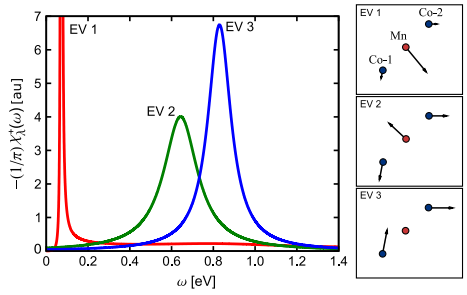

FIG. 1 (color online). Enhanced susceptibility of Co_2MnSi, an example of the spectrum of loss tensor for $\mathbf{q} = 0.28(1, 1, 0)2\pi/a$. a stands for the lattice constant. Three clear peaks (EV 1, 2, and 3 corresponding to the labels in Fig. 2) can be discerned. The panels show corresponding eigenvectors; arrows indicate the deviations of magnetic moments. The basis atoms are Co at $(a/4, a/4, a/4)$ and $3(a/4, a/4, a/4)$ and Mn at $(a/2, a/2, a/2)$.

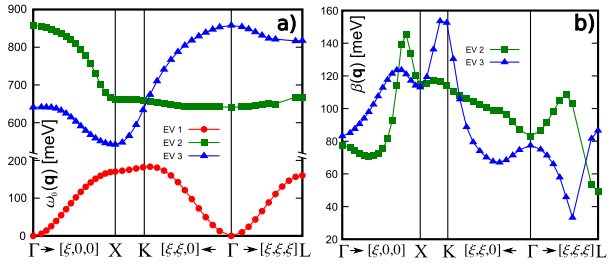

FIG. 2 (color online). Energies (a) and inverse lifetimes (b) of three SW modes in Co_2MnSi. Parameter $\beta_1(\mathbf{q})$ of EV 1 does not exceed 5 meV and it is not shown.

ceed 5 meV for energies above γ_S, even though Landau damping is not excluded there. We notice, however, that γ_S is only the lowest bound for the activation energy of Stoner states and the energy depends strongly on $\mathbf{q}$; additionally, we observe that the density of the KS continuum remains very small up to 270 meV. On the contrary, the "optical" modes (EV 2 and 3) appear where the continuum density is not small and have significant width, which depends strongly and nonmonotonically on $\mathbf{q}$.

The shapes of the excitations corresponding to the three SWs are characterized by an almost rigid rotation of magnetization around atomic sites and the number of SW modes corresponds to the number of magnetic atoms in the primitive cell. Therefore, Co_2MnSi—up to the damping—is a typical Heisenberg Hamiltonian system. In the EV 1 mode the atomic moments oscillate in phase, roughly given by $e^{i\mathbf{q}\cdot\mathbf{r}_i}$, where $\mathbf{r}_i$ stands for the position of atom i. This justifies the use of customary term *acoustic*. For the optical modes some of the moments align themselves roughly in the antiphase to the others, leading to quite intricate shapes of the excitations. As an example, let us consider direction ΓK. The almost dispersionless mode EV 2 formed by Co and Mn moments, cf. Fig. 1, can be regarded as an optical counterpart to EV 1, where Mn moments acquire an additional phase of π. Mode EV 3 involves only Co moments.

We move to the properties of NiMnSb, which is a semi-Heusler half-metallic phase [3,11]. In this system an induced magnetic moment of $0.25\mu_B$ appears on the Ni site due to the hybridization with the states of neighboring Mn atoms [4]. When the Ni moment is treated as an independent Heisenberg degree of freedom it leads to a formation of a soft, weakly dispersive SW branch [12], which is in a disagreement with experiment [13]. While in the Heisenberg model the behavior of the induced moments can be reproduced only by adopting certain empirical assumptions, the LRDFT offers a more fundamental description. In the case of NiMnSb, we observe that in the magnon energy range the loss tensor has only one eigenvalue of significant magnitude. The analysis of the corresponding eigenvector shows that this SW mode is dominated by the dynamics of Mn sublattice, with Ni moments assuming directions along the molecular field coming from Mn atoms.

In order to illuminate the difference in behavior between NiMnSb and Co_2MnSi, we recall that the formation of SW requires that an eigenvalue of $1 - \chi^+_{\mathrm{KS}} K_{\mathrm{xc}}$ becomes small. Since the kernel K_{xc} is frequency independent and rather similar for different $3d$ elements, the formation of SW is determined primarily by features of the unenhanced susceptibility χ^+_{KS}. We notice that for NiMnSb, in the whole interesting energy range, the blocks of susceptibility associated with Ni sites are roughly an order of magnitude smaller than those associated with Mn. The property can be traced back to the small xc interaction on the Ni site, being consistent with the observation that the small moment of Ni arises only due to the Ni-Mn hybridization. As a consequence the second SW branch does not appear. On the contrary, in the Co_2MnSi case the Co-Co and Co-Mn blocks are of comparable magnitude and each magnetic sublattice leads to a separate SW branch.

According to our calculations, at 0 K the only magnon branch of NiMnSb appears entirely in the gap of Stoner continuum ($\gamma_S = 163$ meV), which excludes Landau damping. The comparison of the calculated SW dispersion and available neutron scattering data [13] shows that both have similar $\mathbf{q}$ dependence. There are, however, important differences. The experiment reports that the lifetimes of SWs decrease substantially for energy transfers larger than 60 meV. Additionally, the detected magnons are much softer; cf. Fig. 3. We attribute this difference, first, to the effect of temperature $T = 300$ K of the experiment and, second, to the presence of defects in the sample.

To get insight into temperature dependence of the SW dispersion we performed calculations on the basis of the disordered local moment (DLM) picture [14,15], where the system at $T > 0$ is represented as an alloy $(\mathrm{NiMn})^{\uparrow}_{1-x}(\mathrm{NiMn})^{\downarrow}_{x}\mathrm{Sb}$ of up and down moments described in the coherent potential approximation. The effective moment $M(x)$ can be used to gauge the temperature using the measurements of $M(T)$ of Ref. [11]. The adiabatic magnons calculated for different values of x (and thus T) are presented in Fig. 3. The thermal disorder leads to a decrease of effective interaction between atomic moments and to softening of the magnons. At 300 K the SW stiffness

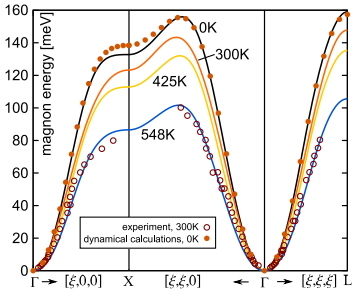

FIG. 3 (color online). Energy of the only spin wave mode in NiMnSb extracted from dynamical susceptibility is compared to experiment [13] and adiabatic SW calculations (solid lines) based on the DLM state, as described in the text.

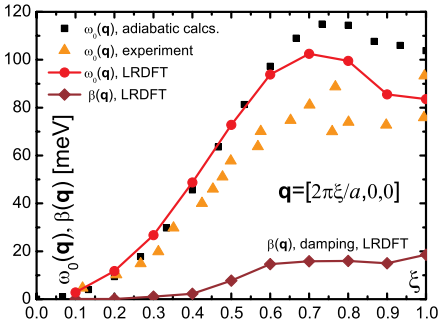

FIG. 4 (color online). Energies (●) and inverse lifetimes (◆) of the SW mode in Cu_2MnAl along the [100] direction obtained in this study compared to the experimental (▲) [20] and adiabatic SW energies (■) [19].

constant decreases by about 10% comparing to 0 K, while the value of 12% was reported in Ref. [11]. The upper part of the experimental spectrum could be reproduced only assuming a much higher temperature of 548 K.

The adiabatic calculation of the temperature dependence neglects the influence of Stoner excitations. At any nonzero temperature the system looses its half-metallicity that leads to the decay of SWs to the low energetic Stoner states absent at 0 K. This leads to the damping observed in the experiment and can result in the renormalization of SW energies, as we will show below on the example of Cu_2MnAl. An experimental study of SW dispersion relation at small temperatures would help to clarify this point and asses the importance of other than Landau-type decay mechanisms. Similarly, the presence of defects leads to a modification of electronic structure and can diminish the interatomic exchange interaction; a study of different samples could be helpful in the latter case.

Recently, a strong temperature dependence of the measured tunneling magnetoresistance (TMR) ratio in tunnel junctions $Co_2MnSi/Al\text{-}O/Co_2MnSi$ has been reported [2]. The type of magnetic excitations responsible for this dependence remains the matter of debates. Chioncel *et al.* [16] suggested the so-called nonquasiparticle states as the leading mechanism, but the measurement of the temperature dependence of the valence band spectrum [17] did not confirm this suggestion. The extension of the present work to the study the magnetic excitations at $Co_2MnSi/Al\text{-}O$ interface can give an important insight into the problem. Also our recent finding [18] that the longitudinal fluctuations of the atomic moments can be a possible mechanism of the strong decrease of the electron spin polarization at the Fermi level without significant change of the total magnetization can be relevant for this problem.

The last system we consider here is non-half-metallic Cu_2MnAl [19]. It features only one magnetic sublattice and therefore only one, acoustic SW mode. The mode hybridizes with Stoner excitations already at small energies since these states do not have an activation energy related to half-metallicity. This simple case allows for a closer look at the influence of the Stoner excitations on the SW energies. The Stoner excitations lead to a clear renormalization of magnon energies compared to the adiabatic treatment, cf. Fig. 4, and the correction brings the theoretical energies closer to the experimental values [20]. Already relatively soft magnons are damped, but the attenuation is much weaker than, e.g., in the case of bcc Fe [7], because the hybridization between transition metal atoms, which in some cases can lead to the opening of the semimetallic gap [4], results also in non-HM Heusler compounds in small density of low energy Stoner states.

In summary, the analysis of dynamic susceptibility improves the description of the low-temperature spin dynamics in complex metallic magnets. It takes into account effects which in the adiabatic studies can be included only on an empirical level (behavior of induced moments) or are completely missing (Landau damping and energy renormalization due to the hybridization with Stoner continuum). In half-metallic ferromagnets the low energy SWs cannot decay into Stoner pairs and can coexist with strongly damped high energy optical magnons.

This work is supported by the *Sonderforschungsbereich* SFB 762, "Functionality of Oxidic Interfaces." Part of the calculations was performed at Rechenzentrum Garching of the Max Planck Society (Germany).

*Corresponding author.
pbuczek@mpi-halle.mpg.de

[1] I. Žutić, J. Fabian, and S. Das Sarma, Rev. Mod. Phys. **76**, 323 (2004).
[2] Y. Sakuraba *et al.*, Appl. Phys. Lett. **88**, 192508 (2006).
[3] R. A. de Groot *et al.*, Phys. Rev. Lett. **50**, 2024 (1983).
[4] I. Galanakis, P. H. Dederichs, and N. Papanikolaou, Phys. Rev. B **66**, 134428 (2002); **66**, 174429 (2002).
[5] S. V. Halilov *et al.*, Phys. Rev. B **58**, 293 (1998).
[6] E. Gross and W. Kohn, Phys. Rev. Lett. **55**, 2850 (1985).
[7] S. Y. Savrasov, Phys. Rev. Lett. **81**, 2570 (1998).
[8] J. B. Staunton *et al.*, Phys. Rev. Lett. **82**, 3340 (1999).
[9] P. Buczek *et al.*, J. Magn. Magn. Mater. (to be published).
[10] S. Ishida *et al.*, J. Phys. Soc. Jpn. **64**, 2152 (1995).
[11] C. Hordequin, J. Pierre, and R. Currat, J. Magn. Magn. Mater. **162**, 75 (1996).
[12] L. M. Sandratskii, R. Singer, and E. Şaşioğlu, Phys. Rev. B **76**, 184406 (2007).
[13] C. Hordequin, J. Pierre, and R. Currat, Physica (Amsterdam) **234–236B**, 605 (1997).
[14] B. L. Gyorffy *et al.*, J. Phys. F **15**, 1337 (1985).
[15] M. Ležaić *et al.*, Phys. Rev. Lett. **97**, 026404 (2006).
[16] L. Chioncel *et al.*, Phys. Rev. Lett. **100**, 086402 (2008).
[17] K. Miyamoto *et al.*, Phys. Rev. B **79**, 100405(R) (2009).
[18] L. M. Sandratskii, Phys. Rev. B **78**, 094425 (2008).
[19] E. Şaşıoğlu, L. M. Sandratskii, and P. Bruno, Phys. Rev. B **77**, 064417 (2008).
[20] K. Tajima *et al.*, J. Phys. Soc. Jpn. **43**, 483 (1977).